Pure and Applied Geophysics

CrossMark

Re-estimate of Major Earthquake Activity in Surrounding Areas after the M_S 6.6 Jinghe Earthquake in Xinjiang, 2017

CHANGLONG LI[1]

Abstract—According to theory, earthquakes may produce disturbances in surrounding areas and affect the major earthquake occurrence rate of surrounding faults. The M_S 6.6 Jinghe Earthquake on 9th August, 2017 occurred in the Tienshan Seismic Belt where there is much tectonic activity and many strong earthquakes occur. The impact of this earthquake on major earthquake activity of surrounding areas is worth studying. This paper attempts to combine two models: the Brownian passage-time (BPT) model, which describes the quasi-periodic recurrence of major earthquakes, and the Coulomb Failure Stress model, which describes rock failure on faults. The amount of change in the rate of major earthquake occurrence caused by a nearby earthquake was calculated, and changes in major earthquake activity in the surrounding areas after the Jinghe Earthquake were re-estimated. There are few differences in major earthquake occurrence rate change by stress disturbances calculated with the BPT model or the Coulomb Failure Stress model. Calculation results are consistent with actual earthquake cases. The 2017 Jinghe Earthquake increased major earthquake activity on the Boluokenu Fault and Yili Basin North Fault, and the expected major earthquake recurrence times of the two faults were advanced by 11 years and 59 years, respectively. Conclusions of this paper provide a reference for time-dependent seismic hazard assessments in related areas.

Key words: Major earthquake occurrence rate, Brownian passage-time model, coulomb stress, time-dependent seismic hazard assessment.

1. Introduction

Reid ([1910](#)) first introduced the Elastic Rebound Theory, which indicated that major earthquake recurrences are quasi-periodic from the perspective of earthquake energy accumulation and release. Many seismologists further developed studies of major earthquake occurrence rates. Shimazaki and Nakata ([1980](#)) introduced the time-predictable and slip-predictable models of major earthquake recurrence and developed methods to evaluate earthquake occurrence rates for different types of models. Schwartz and Coppersmith ([1984](#)) introduced the characteristic earthquake concept, which describes a fault's strongest earthquake recurrence periodically at the same site, with nearly the same magnitude and t focal mechanism. Matthews et al. ([2002](#)) introduced the Brownian passage-time (BPT) model from the perspective of fault stress accumulation rate. This model describes how stress accumulates at a nearly constant rate, but an abrupt disturbance (caused by a nearby earthquake) may advance or postpone the recurrence of major earthquakes and lead to changes in earthquake occurrence rate.

Concurrently, some seismologists have studied fault interactions and earthquake triggering. Most studies on faults are based on Coulomb Failure Stress. Many studies have focused on the correlation of Coulomb Failure Stress change and earthquake occurrence rate change (Stein et al. [1994](#), [1997](#); Toda et al. [1998](#), [2005](#), [2008](#); Stein [1999](#); Toda and Stein [2002](#), [2003](#); Ma et al. [2005](#); Parsons et al. [2008](#)). These studies calculate Coulomb Failure Stress change for an earthquake and evaluate qualitatively if it triggered a nearby earthquake. Dieterich ([1994](#)) studied stress disturbance and earthquake occurrence rate and developed a quantitative relationship between stress change and change of earthquake occurrence rate over time.

Consequently, it has been widely recognized that earthquakes may produce disturbances in surrounding areas and change the major earthquake occurrence rate of surrounding faults. There have been many studies on quasi-periodic earthquake recurrence

[1] Institute of Geophysics, China Earthquake Administration, No. 5 Minzu Daxue Nanlu Road, Beijing 100081, China. E-mail: changlongli@163.com

models and Coulomb Failure Stress impacts on earthquake occurrence rates. The impact of a nearby earthquake on the earthquake occurrence rate can be obtained through either the BPT or the Coulomb Failure Stress models. But the relationship between the two models and calculation confidence are worth studying.

On 9th August, 2017, an M_S 6.6 earthquake occurred in Jinghe, Xinjiang, China. The earthquake destroyed a small number of houses, but no people were severely injured because the population is sparse. This earthquake happened in the Tienshan Seismic Belt, where there is frequent tectonic activity and strong earthquakes occur. So the impact of this earthquake on major earthquake activity of the surrounding areas is worth studying. This paper attempts to combine two models to determine changes in major earthquake occurrence rates. The BPT model describes the quasi-periodic recurrence of major earthquakes, and the Coulomb Failure Stress model describes rock failure on faults. The amount of change in the major earthquake occurrence rate caused by a nearby earthquake was calculated, and the expected major earthquake recurrence time of surrounding faults was re-estimated. Because major earthquake occurrence rate is an important factor in seismic hazard assessment, the conclusions of this paper will be useful for time-dependent seismic hazard assessment in related areas.

2. Study on Stress Disturbance Impact on Earthquake Occurrence Rate

The impact of a nearby stress disturbance on earthquake occurrence rate can be calculated by the BPT model or the Coulomb Failure Stress (CFS) model. Both models consider loading or unloading by a nearby earthquake on fault stress, which causes seismicity changes.

2.1. Brownian Passage-Time (BPT) Model

Matthews et al. (2002) improved the Elastic Rebound Theory (Reid 1910) and developed the BPT model describing major earthquake recurrences on faults. This model assumes that after a fault's strongest

(or nearly strongest) earthquake, the fault will begin a new cycle of major earthquake stress accumulation and recurrence, and the expression of the fault state $\dot{X}$ (which can be described with the stress loading rate or fault deformation rate) is shown as

$$\dot{X} = \lambda + \sigma \dot{W}, \tag{1}$$

In which λ is the fault state loading rate, $\dot{W}$ is standard Brownian random movement, and σ is a constant coefficient between 0 and 1 to describe the strength of the impact of Brownian movement on fault state.

The BPT model posits that, for a certain fault, major earthquake recurrence is periodic, which is described as constant loading rate λ, and $\dot{X}$ describes a fault's state in its major earthquake recurrence cycle. Small earthquakes and nearby earthquakes are random, loading and unloading the fault state continually. This type of disturbance is described by weighted Brownian movement, $\sigma \dot{W}$ ($0 \leq \sigma \leq 1$). The larger the σ, the more uncertainty in major earthquake occurrences.

The probability density function of major earthquake occurrence in the BPT model is expressed as

$$f(t) = \sqrt{\frac{\mu}{2\pi\alpha^2 t^3}} \exp\left[-\frac{(t-\mu)^2}{2\alpha^2\mu t}\right], \tag{2}$$

In which μ is the average major earthquake recurrence period and α is the uncertainty in major earthquake recurrence, which is expressed as

$$\alpha = \frac{\sigma}{\lambda\sqrt{\mu}} \tag{3}$$

The major earthquake occurrence probability P in a time window ($T_e \sim T_e + \Delta T$) can be calculated as

$$P = \frac{\int_{T_e}^{T_e+\Delta T} f(t)\mathrm{d}t}{1 - \int_0^{T_e} f(t)\mathrm{d}t}, \tag{4}$$

Which means that if we know the average slip rate of a fault, major earthquake recurrence cycle, the disturbance strength ratio between major and small earthquakes, and when the last major earthquake occurred, we can calculate the major earthquake occurrence rate in a certain time window. Specifically, when we take $\Delta T = 1$, P is the annual rate of major earthquakes.

2.2. The Delay Effect of a Disturbance on Major Earthquake Occurrences

The BPT model points out that an abrupt disturbance may change major earthquake recurrence times (Fig. 1). An unloading disturbance may delay recurrence time (Fig. 1a), while a loading disturbance may advance the time (Fig. 1b). If the fault state is loaded to critical, a major earthquake will be triggered directly (Fig. 1c). When the fault is quite long, different segments may have different stress states. In this case fault segments can be considered separately. Figure 1a indicates the case where a small earthquake occurs on the fault or an unloading earthquake occurs nearby, Fig. 1b shows a loading earthquake that occurs nearby, and Fig. 1c shows that a critical loading triggers a major earthquake.

Calculation of the delay time of a major earthquake by stress disturbance can be done with the seismic moment release rate method (Wensnousky 1986). Assuming the seismic moment of a major earthquake is M, the recurrence period is T and the moment of a small earthquake on the fault is M', then the delay time Δt can be calculated as
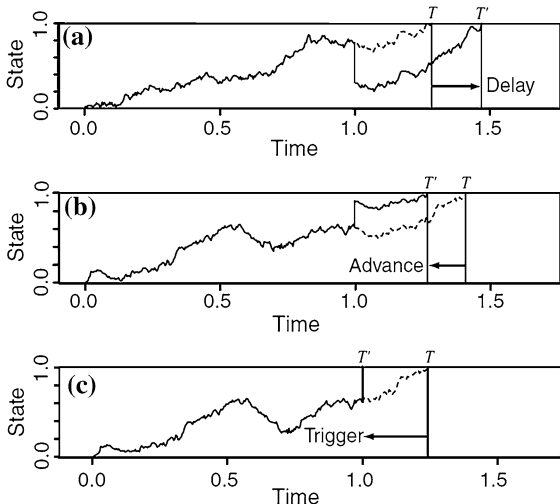
$$\Delta t = \frac{M'}{M} T \qquad (5)$$

Figure 1
The influence of stress disturbance on fault state. **a** Disturbance delays the recurrence of a major earthquake; **b** disturbance advances the recurrence of a major earthquake; **c** disturbance advances the fault state to critical and triggers a major earthquake. (Matthews et al., 2002)

For earthquakes with no way to measure seismic moments, we can use the empirical relationship between magnitude and moment. The relationship was developed by Hanks and Kanamori (1979), as

$$M_{\mathrm{w}} = \frac{2}{3} \lg M_0 - 10.7, \qquad (6)$$

In which M_0 is seismic moment and M_{W} is the corresponding moment magnitude.

After obtaining Δt, in combination with Eq. (2), the probability density function of major earthquake recurrence changes to

$$f(t - \Delta t) = \sqrt{\frac{\mu}{2\pi\alpha^2 t^3}} \exp\left[-\frac{(t-\mu)^2}{2\alpha^2\mu t}\right] \qquad (7)$$

Which assumes that the fault state has recovered to Δt years prior to the earthquake and then accumulates in its original way.

2.3. Stress Disturbance Impacts on Major Earthquake Occurrence Rates

Research shows that rock failure during an earthquake follows the Coulomb failure criterion (Jaeger and Cook 1969). An earthquake can cause changes to Coulomb Failure Stress on its fault and surrounding areas. Coulomb Failure Stress is defined as

$$\Delta\mathrm{CFS} = \Delta\tau + \mu\Delta\sigma_n \qquad (8)$$

In which $\Delta\mathrm{CFS}$ is Coulomb Failure Stress change. $\Delta\tau$ is shear stress change, which is positive in the same direction of the fault slip. μ is the friction coefficient, and $\Delta\sigma_n$ is normal stress change, where tensile stress is positive.

Dieterich (1994) developed an equation showing the relationship between stress disturbance and seismicity $R(t)$ with time t, as

$$R(t) = \frac{r}{\left[\exp\left(\frac{-\Delta\sigma_j}{A\sigma}\right) - 1\right]\exp\left(\frac{-t}{t_a}\right) + 1} \qquad (9)$$

In which r is seismicity before the disturbance. $\Delta\sigma_j$ is stress change, A is the fault structure parameter, and σ is normal stress; for a certain fault, $A\sigma$ is constant.

Combining Eqs. (4) and (9), in the T_nth year after a stress disturbance, the major earthquake occurrence rate P_n is

$$P_n = \frac{\int_{T_n}^{T_n+1} f(t)\mathrm{d}t}{\left[1 - \int_0^{T_n} f(t)\mathrm{d}t\right]\left\{\left[\exp\left(\frac{-\Delta\sigma_j}{A\sigma}\right) - 1\right]\exp\left(\frac{-T_n}{t_a}\right) + 1\right\}}$$

(10)

In which the parameters are defined as in Eqs. (4) and (9). Then we can calculate the major earthquake occurrence rate change for every year after a disturbance.

3. Method Tested by Two Examples

According to the introduction, the impact of a small earthquake on the major earthquake occurrence rate of a fault can be calculated through the BPT model or the Coulomb Failure Stress model. But the two methods are based on different theories, so it is necessary to compare the respective results. However, we cannot calculate the major earthquake occurrence rate change caused by a nearby disturbance with the BPT model, but can get it indirectly through the Coulomb Failure Stress model. The result calculated by the Coulomb Failure Stress model can be tested by historical earthquake examples. This section takes two examples from the Xianshuihe Fault in the eastern part of the Tibetan Plateau, China, to test the method of combining the Coulomb Failure Stress and BPT models to calculate changes in the major earthquake occurrence rate.

Strong earthquakes occur frequently on the Xianshuihe Fault and seismologists are deeply concerned with its seismic hazards. Surface deformation and geodesy data applied to fault movement features, slip rates, and stress disturbance impacts on surrounding faults are the main aspects of current studies on the Xianshuihe Fault. For example, Li et al. (2015) analyzed deformation features of the Bamei-Daofu section of Xianshuihe Fault from 2007 to 2011 with permanent scatterer interferometric synthetic aperture radar (InSAR) data. Fang et al. (2015) analyzed movement features of the northwestern section of the Xianshuihe Fault with cross-fault deformation data, and measured fault slip rate. Wang et al. (2009) studied interseismic slip rates of the Xianshuihe Fault with InSAR data. Su et al. (2012) studied strong earthquake predictive indexes of the Xianshuihe Fault

from cross-fault observation data, and summarized the relationship between strong earthquake occurrence and prognostic abnormalities. Zhang et al. (2012) studied activity of the Xianshuihe Fault and relationships with large earthquakes based on Grey relational analysis. These studies are helpful to build the BPT model of major earthquake recurrence on the Xianshuihe Fault.

The impact of historical earthquakes on Coulomb Failure Stress on the Xianshuihe Fault is also a hot issue (Zhang et al. 2003; Wang et al. 2009; Xu et al. 2013; Wu et al. 2014). These studies mainly focus on the relationship between the Coulomb Failure Stress triggering threshold and occurrence of major earthquakes in related areas. The results of these studies can also be used to quantitatively study the impact of Coulomb Failure Stress on the occurrence rate of large earthquakes. For example, Liu et al. (2013) studied changes in the seismicity of the Xianshuihe Fault caused by the 2008 M7.9 Wenchuan earthquake and the 2013 M7.0 Lushan earthquake.

Strong earthquakes have occurred frequently on the Xianshuihe Fault in the last 300 years (Fig. 2, Yi et al. 2015). The 1981 M6.9 Daofu earthquake and the 1967 M6.8 Zhuwo earthquake are taken as examples. The impacts of both earthquakes on major earthquake occurrence rates of related faults are calculated, and the reliability of combining the BPT and Coulomb Failure Stress models is analyzed.

3.1. The Impact of the 1981 M6.9 Daofu Earthquake on the Daofu-Qianning Section of the Xianshuihe Fault

The BPT model was applied to the 1981 M6.9 earthquake on the Daofu-Qianning Section of the Xianshuihe Fault. The slip rate of the Xianshuihe Fault is 9 mm/a to 12 mm/a (Zhou et al. 2001; Wang et al. 2009; Fang et al. 2015; Yi et al. 2015). In this work it is considered as 12 mm/a. The largest historical earthquake on this section is the 1893 M7.25 earthquake (Wen 2000). So the maximum magnitude of this section is set at 7.5.

According to the relationship between magnitude and coseismic displacement (Wells and Coppersmith 1994), in combination with related research on major earthquake coseismic displacement on the
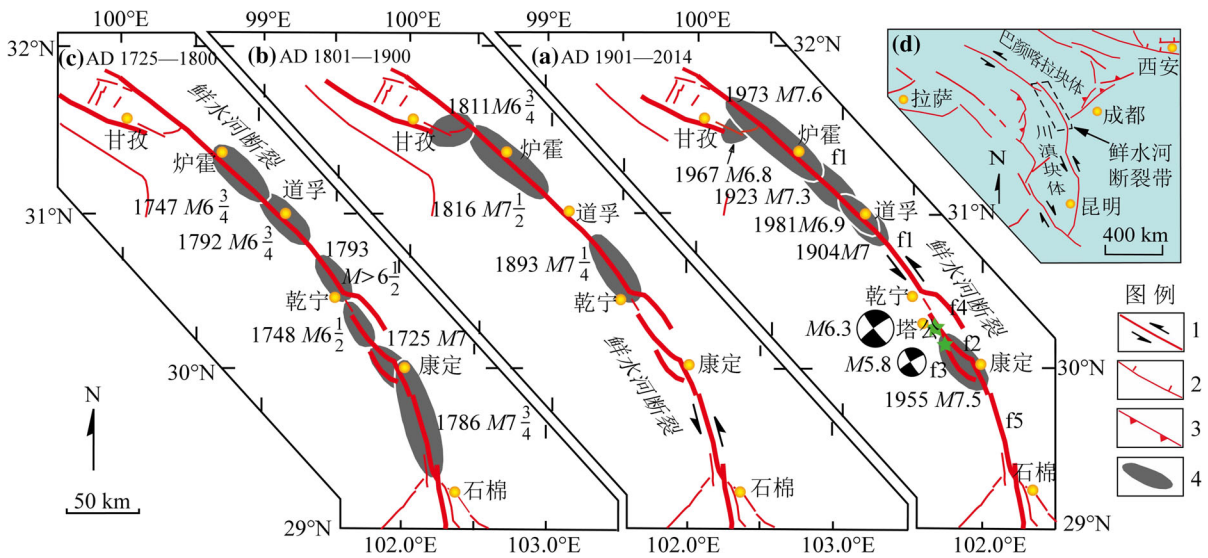
Figure 2
Historical earthquakes on the middle and southern parts of the Xianshuihe Fault (Yi et al. 2015). 1, Strike slip fault. 2, Normal fault. 3, Reverse fault. 4, Historical earthquake rupture zones. f1: Xianshuihe Fault. f2: Selaha Fault. f3: Zheduotang Fault. f4: Yalahe Fault. f5: Moxi Fault

Xianshuihe Fault (Zhou et al. 1983a, b), we can ascertain that an M7.5 earthquake has an average displacement of 2 m to 4 m. In this work it is considered 3 m. Combining this with the annual slip rate, the recurrence cycle of an M7.5 earthquake is calculated as 250 years (3 m divided by 12 mm/a = 250 a).

According to the empirical equation for moment magnitude (Hanks and Kanamori 1979), the 1893 M7.25 earthquake moment is about 3×10^{19} N/m². The 1981 M6.9 Daofu earthquake moment is about 8×10^{18} N/m² (Zhou et al. 1983a; Papadimitriou et al. 2004). From Eqs. (2) and (3), $\lambda = 0.012$ m/a, $\mu = 250$ a, and $\sigma = [(8 \times 10^{18}$ N/m²$)/(3 \times 10^{19}$ N/m²$)] = 0.27$. The probability density function for a major earthquake on the Daofu-Qianning Section is shown in Fig. 3.

Assuming the Daofu-Qianning Section started a new recurrence cycle for an M7.5 earthquake from 1893, the elapsed time would be 88 years when the 1981 earthquake occurred. According to Eqs. (2) and (4), the major earthquake occurrence rate in 1981 before the M6.9 earthquake was 8.6×10^{-6}. After the 1981 earthquake, the fault state was unloaded, as shown in Fig. 1a. From Eq. (5), the expected time delay of a major earthquake can be calculated as

$\sigma \cdot \mu = 67$ years. Then from Eq. (7), the probability density function for a major earthquake can be calculated as the dotted line in Fig. 3.

The 1981 M6.9 Daofu earthquake decreased the Coulomb Failure Stress by about 0.3 MPa on the Daofu-Qianning Section (Zhang et al. 2003). The major earthquake occurrence rate change year by year can be calculated for this section using Eq. (10).

Figure 4 shows the major earthquake occurrence rate change year by year for the Daofu-Qianning Section, calculated by the BPT model and Coulomb Stress model, respectively. As can be seen from the figure, after the M6.9 earthquake in 1981 (when the elapsed time was 88 years), the annual major earthquake occurrence rate was significantly reduced for both models. Within 100 years after the 1981 earthquake, the major earthquake occurrence rates are not much different.

3.2. The Impact of the 1967 Zhuwo M6.8 Earthquake on the Ganzi-Luhuo Section of the Xianshuihe Fault

In 1967, an M6.8 earthquake occurred in Zhuwo (Fig. 2). Only 6 years after this earthquake, in 1973, an M7.6 earthquake occurred in Luohuo, southeast of
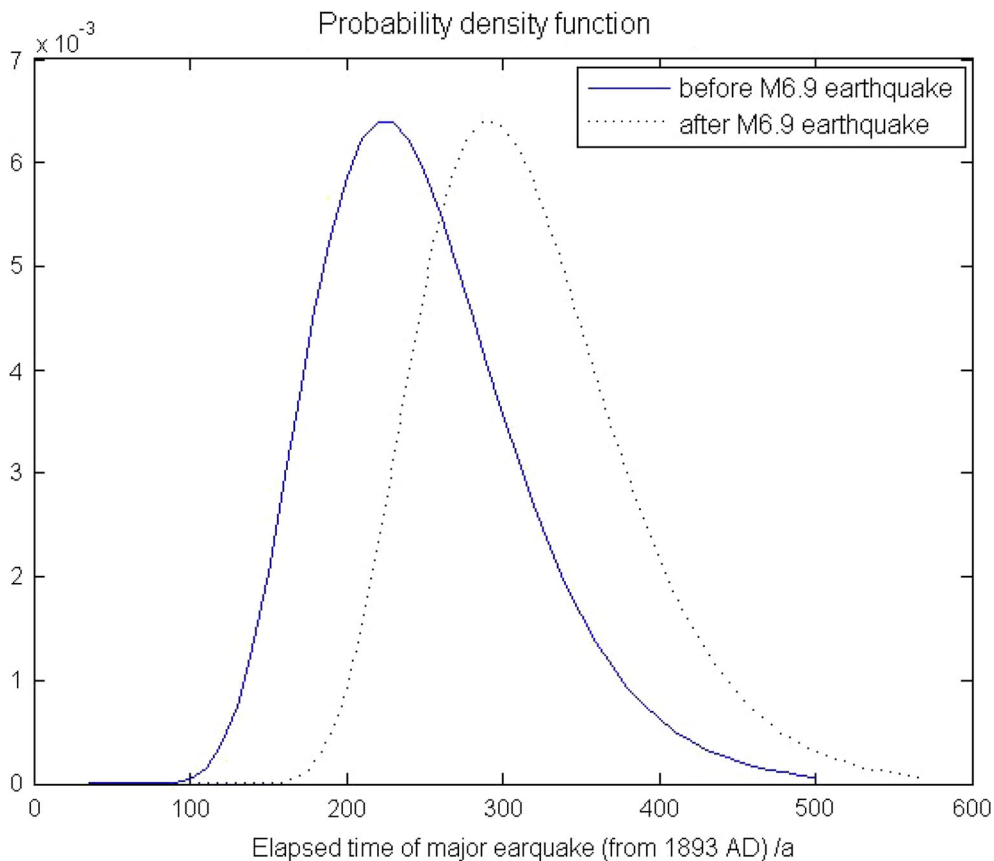
Figure 3
Probability density functions for a major earthquake on Daofu-Qianning Section before and after the M6.9 earthquake in 1981

Zhuwo. The impact of the Zhuwo earthquake on the Ganzi-Luhuo Section is worth studying.

A historical M7.5 earthquake occurred in 1816 on the Ganzi-Luhuo section. The BPT model for this section can be described according to the method given in Sect. 2.1. The average slip distance of a major earthquake is assumed as 3 m (Zhou et al. 1983a, b), and the major earthquake recurrence cycle is about 250 years. The annual major earthquake occurrence rate change year by year is shown as a solid line in Fig. 5. In 1967, before the Zhuwo earthquake, the elapsed time since a major earthquake was 151 years, and the annual major earthquake rate was about 0.0022.

The 1967 earthquake increased Coulomb Failure Stress by 0.05 to 0.1 MPa on the Ganzi-Luhuo Section (Zhang et al. 2003), and in this work the increase is considered 0.08 MPa. The annual major earthquake rate changed to 0.0142 after the 1967 earthquake. The annual changes of major earthquake rate calculated by the Coulomb Failure Stress model and the BPT model are shown in Fig. 5.

The change in expected major earthquake occurrence time can be calculated using the change of major earthquake rate in combination with the BPT model. From Fig. 5, the annual rate of 0.0142 corresponds to a major earthquake elapsed time of 261 years, which exceeds the major earthquake cycle of 250 years. This means the fault has been loaded to the critical state, and a major earthquake may occur at any time. That is to say, compared with the Coulomb Failure Stress model, the expected time of the next major earthquake with the BPT model was advanced, by about (250 − 151 =) 99 years.

In fact, only 6 years after the Zhuwo Earthquake, an M7.6 earthquake occurred on the Ganzi-Luhuo
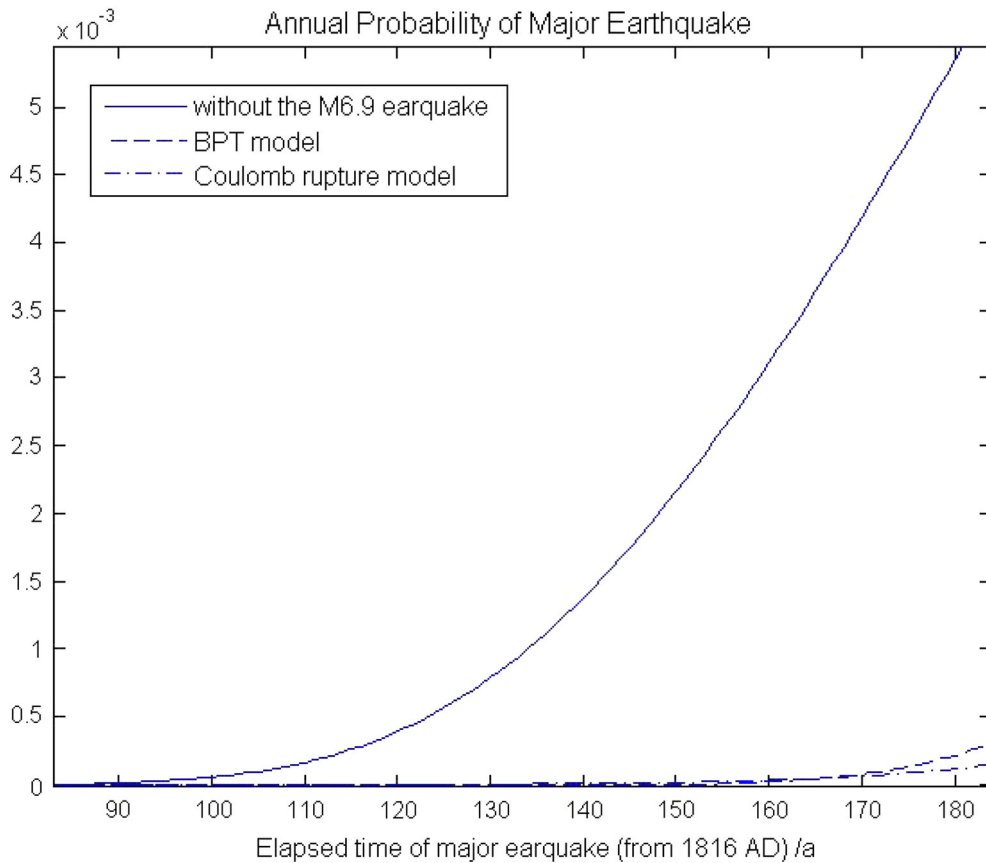
Figure 4
Annual probabilities of a major earthquake on the Daofu-Qianning Section after the 1981 M6.9 earthquake, computed by the BPT and Coulomb Failure Stress model

Section, which was (2066 − 1973 =) 93 years earlier than the original expected time, 2066 (1816 + 250). Table 1 shows the comparison between Ganzi-Luhuo Section states calculated by models and in reality. The results calculated by models are in accordance with reality.

4. The Impact of the 2017 M6.6 Jinghe Earthquake on Major Earthquake Activity of Surrounding Areas

Combining the BPT model and Coulomb Failure Stress model according to Sect. 2 to calculate the major earthquake occurrence rate change is reliable for the selected examples. Here, the method is applied to the 2017 M6.6 Jinghe Earthquake and surrounding areas.

After comprehensive analysis of the epicenter location and earthquake tectonic map (Fig. 6), the seismogenic fault is identified as the Kusongmuqike Fault. An M7.2 earthquake occurred in 1944 on the Boluokenu Fault to the east of the Jinghe Earthquake, and an M8 earthquake occurred in 1812 on the Yili Basin North Fault to the south of the Jinghe Earthquake. As both faults are very long and have different slip behaviors on different segments, the two faults considered here are limited to their corresponding segments near the epicenters of the last major earthquakes.

The major earthquake elapsed time for the Boluokenu Fault is 73 years. The maximum magnitude of the Boluokenu Fault is considered 7.5, and the major
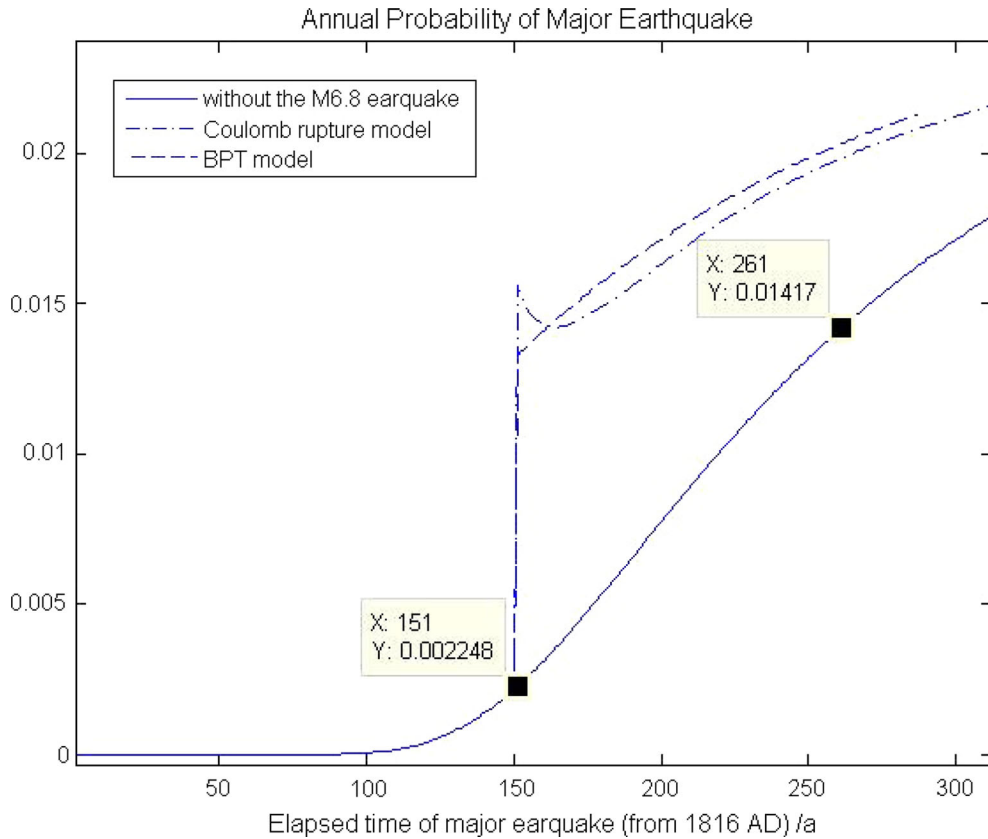
Figure 5
Annual probabilities of a major earthquake on the Ganzi-Luhuo Section after the M6.8 earthquake in 1967 computed by the BPT and Coulomb Failure Stress models

Table 1

Probabilities of major earthquake on Ganzi-Luhuo Fault before and after the 1967 M6.8 Zhuwo earthquake

	Calculated by model		Reality
	Before the 1967 earthquake	After the 1967 earthquake	
Major earthquake occurrence rate	0.0022	0.0142	
Year of major earthquake occurrence	2066	1967	1973
Advanced years of major earthquake	99		93

earthquake displacement is taken as 3 m. The fault slip rate is assumed as 7.6 mm/a (Shen et al. 2011), and the major earthquake recurrence cycle is estimated as 395 years. The next major earthquake expected time is (1944 + 395 =) 2339. The σ in Eq. (3) is taken as the seismic moment ratio of M7.2 and M7.5. Then, in Eqs. (2) and (3), $\lambda = 0.0076$ m/a, $\mu = 395$ a, and $\sigma = 0.35$. Before the Jinghe Earthquake, the annual major earthquake occurrence rate of the Boluokenu Fault was about 1.76×10^{-8}. The major earthquake occurrence rate year by year is shown as the solid line in Fig. 7.

The major earthquake elapsed time for the Yili Basin North Fault is 205 years. The maximum magnitude of the Yili Basin North Fault is taken as 8, and major earthquake displacement is set at 4 m. The fault slip rate is assumed as 8.5 mm/a (Shen et al. 2011), and the major earthquake recurrence cycle is estimated as 471 years. The next major earthquake expected time is (1812 + 471 =) 2283. Before the Jinghe Earthquake, the annual major earthquake
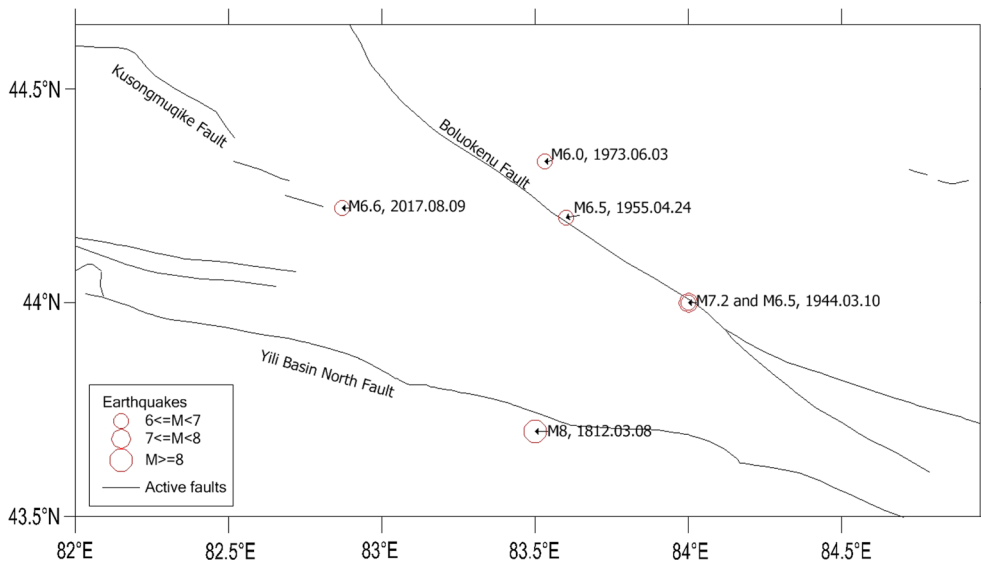
Figure 6
Earthquake tectonic map and historical earthquakes in the area surrounding the 2017 M6.6 Jinghe Earthquake

occurrence rate on the Yili Basin North Fault is about 4.34×10^{-4}. The major earthquake occurrence rate year by year is shown as the solid line in Fig. 8.

The Coulomb Failure Stress change distribution for the Jinghe Earthquake was then calculated with the COULOMB 3 Software developed by Toda et al.

(2011). Seismogenic fault parameters are taken from Shen et al. (2011), and focal parameters are taken from Han (2017). The Coulomb Failure Stress change distribution is shown in Fig. 9.

Figure 9 shows that the 2017 M6.6 Jinghe Earthquake increased the Coulomb Failure Stress of
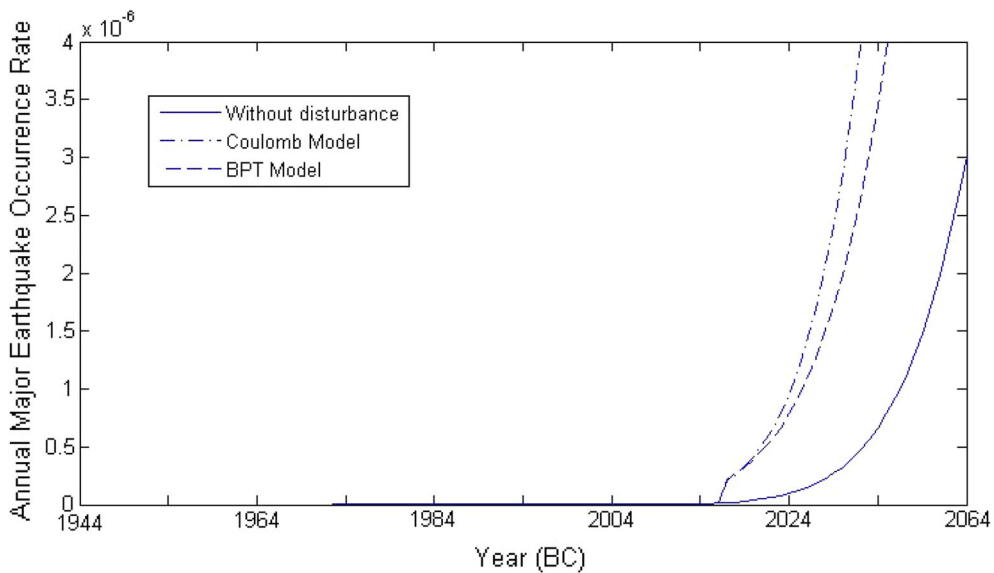

Figure 7
Major earthquake occurrence rate of the Boluokenu Fault before and after the 2017 M6.6 Jinghe Earthquake
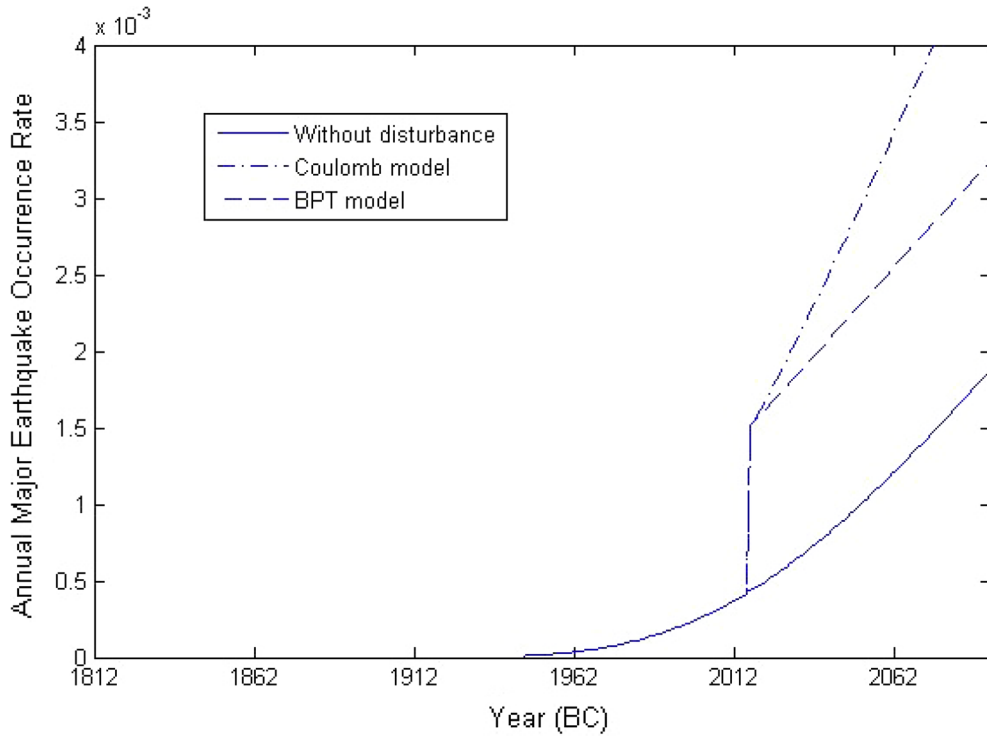
Figure 8
Major earthquake occurrence rate for the Yili Basin North Fault before and after the 2017 M6.6 Jinghe Earthquake
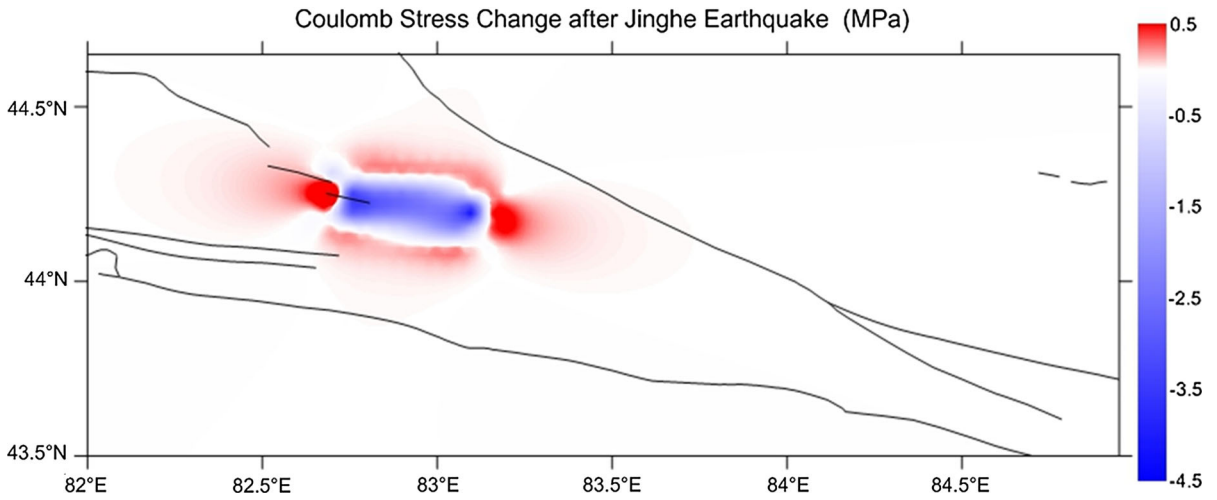

Figure 9
Coulomb Failure Stress change distribution for the 2017 M6.6 Jinghe Earthquake

the Middle Boluokenu Fault by about 0.1 MPa. From Eq. (9), the calculated Coulomb Failure Stress change may increase the major earthquake occurrence rate to about 2.09×10^{-7}. The major earthquake occurrence rate change calculated by the BPT model and the Coulomb model are shown as the

dashed line and dot-dashed line in Fig. 7, respectively.

With the BPT model, the major earthquake elapsed time under an annual rate of 2.09×10^{-7} is about 84 years. That means the expected major earthquake recurrence time is advanced by about $(84 - 73)$ 11 years.

Figure 9 shows that the 2017 M6.6 Jinghe Earthquake made the Coulomb Failure Stress of the Middle Yili Basin North Fault increase by about 0.05 MPa. From Eq. (9), the Coulomb Failure Stress change may increase the major earthquake occurrence rate to about 0.0015. The major earthquake occurrence rate changes calculated by the BPT model and the Coulomb model are shown as a dashed line and a dot-dashed line in Fig. 8, respectively.

With the BPT model, the major earthquake elapsed time under an annual rate of 0.0015 is about 264 years. That means the expected major earthquake recurrence time is advanced by about $(264 - 205)$ 59 years.

5. Conclusion

This paper quantitatively studies the impact of stress disturbances on changes in major earthquake occurrence rates with the BPT and Coulomb Failure Stress models. Several earthquake examples on the Xianshuihe Fault were used to compare calculation results for the two models, and test confidence in this method. Then this method was applied to the re-estimation of major earthquake activity in surrounding areas after the 2017 M6.6 Jinghe Earthquake. The following conclusions are reached:

1. Changes in the major earthquake occurrence rate caused by stress disturbances can be calculated with both the BPT and Coulomb Failure Stress model. Results of the two models have few differences.
2. The major earthquake occurrence rate change calculation results of the two models are consistent with actual earthquake cases. The two models validate each other and have a certain level of confidence.

3. The 2017 M6.6 Jinghe Earthquake increased major earthquake activities on the Boluokenu Fault and Yili Basin North Fault, and the expected major earthquake recurrence times of the two faults were advanced by 11 years and 59 years, respectively.

6. Discussion

The methods and results of this paper raise the following points that are worth discussing:

1. The uncertainties of the models. Parameters in both the BPT and Coulomb Failure Stress models have large uncertainties. Parameter selection will significantly impact calculation results. The relationships between magnitude and slip displacement, the fault slip rate, and the recurrence cycle are considered empirical equations and have large tolerance scopes. Whether the examples and results in this paper have universal significance needs further research to verify.
2. The expected major earthquake recurrence time is defined here as the year in which the elapsed time since a major earthquake equals the recurrence period. Advancing of the expected major earthquake recurrence time increases the major earthquake occurrence rate and seismic hazard. However, the occurrence of a major earthquake is affected by many factors, and seismogenic mechanisms remain uncertain. The advancing of expected major earthquake recurrence time does not mean the recurrence of major earthquakes will certainly come earlier than before.
3. Building models in which there are frequent disturbances. On the Xianshuihe Fault, strong earthquakes occur frequently on different sections. This provides an excellent example to study the relationship between stress disturbance and earthquake activities. However, it makes building the BPT model more difficult because in a single recurrence cycle, fault state may be changed many times by frequent disturbances. In the future, more accurate models will be needed to describe interactions among many earthquakes.

4. Different activity patterns on different faults. Xianshuihe Fault is taken as an example because the method needs actual major earthquake recurrences to test. Further study is needed to check if this method is applicable on all faults.

5. For the BPT model, it is assumed that external loading occurs at a constant rate. The BPT model has some limitations. In actuality, there are two types of loading: gravity and boundary loads on the sides of neighboring blocks (plates). In quasi-plastic flow, this process is not linear. There are also differences when calculating Coulomb Failure Stress using an elastic model or a quasi-plastic model. In future studies, more models should be developed to better describe fault behaviors.

6. Changes in fault state may not be solely because of stress changes in the BPT model. Changes in thermal and fluid regimes in the fault zone may also cause fault state changes. This may need more study in the future.

7. To assume the scale of fault displacement, this paper uses the relationship developed by Wells and Coppersmith (1994). A given fault may have more complex behavior, for example restrictions on the self-similarity condition of faults (Kocharyan et al. 2014). More fault mechanisms should be considered in future studies.

8. In the BPT model, attaining a critical state always ends with a major earthquake (large-scale brittle fracture). In fact, there are many other dissipation mechanisms of excess mechanical energy, such as: earthquakes, silent earthquakes, episodic tremor and slip, episodic creep events, slow slip events, low-frequency earthquakes, or very low-frequency earthquakes (Peng and Gomberg 2010; Sekine et al. 2010; Wei et al. 2009). In this case, the expected frequency of major earthquakes may not prove true, and the periodicity of large-scale dissipation of mechanical energy will persist. The complex behavior of faults and their energy dissipation mechanisms will be the focus of future research.

In this work, research on interactions between earthquakes and faults has been carried out on a large scale, providing new ideas for time-dependent seismic hazard assessment. In the future, more examples and better models should be used to continue relevant research, and enrich time-dependent seismic hazard assessment methods.

7. Data and Resources

The data used in this paper include fault tectonic parameters and seismogenic parameters of several earthquakes. All data and resources have been published in other research and are cited in the text.

References

Dieterich, J. (1994). A constitutive law for rate of earthquake production and its application to earthquake clustering. *Journal of Geology Research, 99*(10), 2601–2618.

Fang, Y., Zhang, J., Jiang, Z. S., Shao, Z. G., & Cao, J. L. (2015). Movement characteristics of the northwest segment of the Xianshuihe fault zone derived from cross-fault deformation data. *Chinese Journal of Geophysics (in Chinese), 58*(5), 1645–1653.

Han, L. B. (2017). Earthquake moment tensor inversion of Xinjiang Jinghe M_S 6.6 Earthquake on 09.08.2017. Earthquake summary poster of Institute of Geophysics, China Earthquake Administration. **(in Chinese)**

Hanks, T. C., & Kanamori, H. (1979). A moment-magnitude scale. *Journal of Geophysical Research, 84,* 2348–2350.

Jaeger, J. C., & Cook, N. G. (1969). Fundamentals of Rock Mechanics. New York.

Kocharyan, G. G., Ostapchuk, A. A., Markov, V. K., et al. (2014). Some questions of geomechanics of the faults in the continental crust. *Izvestiya, Physics of the Solid Earth, 50*(3), 355–366.

Li, L. J., Yao, X., Zhang, Y. S., Wang, G. J., & Guo, C. B. (2015). The extraction of the near-field deformation features along the

faulted zone based on PS-InSAR survey. *Geological Bulletin of China (in Chinese), 34*(1), 217–228.

Liu, B. Y., Shi, B. P., & Lei, J. S. (2013). Effect of Wenchuan earthquake on probabilities of earthquake occurrence of Lushan and surrounding faults. *Acta Seismologica Sinica (in Chinese), 35*(5), 642–651.

Ma, K. F., Chan, C. H., & Stein, R. S. (2005). Response of seismicity to Coulomb stress triggers and shadows of the 1999 Mw7.6 Chi-Chi Taiwan, earthquake. *Journal of Geophysical Research, 110*(5), 82–89.

Matthews, M. V., Ellsworth, W. L., & Reasenberg, P. A. (2002). A Brownian model for recurrent earthquakes. *Bulletin of the Seismological Society of America, 92*(6), 2233–2250.

Papadimitriou, E., Wen, X. Z., Karakostas, V., & Jin, X. S. (2004). Earthquake triggering along the Xianshuihe fault zone of western Sichuan, China. *Pure and Applied Geophysics, 161*(8), 1683–1707.

Parsons, T., Ji, C., & Kirby, E. (2008). Stress changes from the 2008 Wenchuan earthquake and increased hazard in the Sichuan basin. *Nature, 454*(7203), 509–510.

Peng, Z., & Gomberg, J. (2010). An integrated perspective of the continuum between earthquakes and slow-slip phenomena. *Nature Geoscience, 3*(9), 599.

Reid, H. E. (1910). The mechanics of the earthquake. The California Earthquake of April 18, 1906. Report of the State Earthquake Investigation Commission: Carnegie Institution of Washington Publication.

Schwartz, D. P., & Coppersmith, K. J. (1984). Fault behavior and characteristic earthquakes: examples from the Wasatch and San Andreas Fault Zones. *Journal of Geophysical Research Solid Earth, 89*(7), 5681–5698.

Sekine, S., Hirose, H., & Obara, K. (2010). Short-term slow slip events correlated with non-volcanic tremor episodes in southwest Japan. *Journal of Geophysical Research, 115*(B9), B00A27.

Shen J., Bai M. X., & Shi G. L. (2011). Map of Xinjiang Earthquake Tectonics Instructions.

Shimazaki, K., & Nakata, T. (1980). Time-predictable recurrence model for large earthquakes. *Geophysical Research Letters, 7*(4), 279–282.

Stein, R. S. (1999). The role of stress transfer in earthquake occurrence. *Nature, 402*, 605–609.

Stein, R. S., Barka, A. A., & Dieterich, J. H. (1997). Progressive failure on the North Anatolian fault since 1939 by earthquake stress triggering. *Geophysical Journal International, 128*, 594–604.

Stein, R. S., King, G. C., & Lin, J. (1994). Stress triggering of the 1994 M = 6.7 Northridge, California, earthquake by its predecessors. *Science, 265*, 1432–1435.

Su, Q., Yang, Y. L., Wang, L., & Xiang, H. P. (2012). Study on the strong earthquake predictive indexes from the fault-crossing observation data of mobile crustal deformation measurement along the Xianshuihe faults. *Earthquake research in Sichuan (in Chinese), 145*(4), 10–17.

Toda, S., Lin, J., Meghraoui, M., & Stein, R. S. (2008). 12 May 2008 M = 7.9 Wenchuan, China, earthquake calculated to increase failure stress and seismicity rate on three major fault systems. *Geophysical Research Letters, 35*(L17305), 1–6.

Toda, S., & Stein, R. S. (2002). Response of the San Andreas fault to the 1983 Coalinga-Nuñez earthquakes: An application of interaction-based probabilities for Parkfield. *Journal of Geophysical Research, 107*(B6), 6–16.

Toda, S., & Stein, R. S. (2003). Toggling of seismicity by the 1997 Kagoshima earthquake couplet: A demonstration of time-dependent stress transfer. *Journal of Geophysical Research, 108*(B12), 1–12.

Toda, S., Stein, R. S., Sevilgen, V., et al. (2011). Coulomb 3.3 graphic-rich deformation and stress-change software for earthquake, tectonic, and volcano research and teaching-user guide. US Geological Survey.

Toda, S., Stein, R. S., Reasenberg, P. A., Dieterich, J. H., & Yoshida, A. (1998). Stress transferred by the 1995 Mw = 6.9 Kobe, Japan, shock: Effect on aftershocks and future earthquake probabilities. *Journal of Geophysical Research, 103*(10), 24543–24565.

Toda, S., Stein, R. S., Richards-Dinger, K., & Bozkurt, S. B. (2005). Forecasting the evolution of seismicity in southern California: Animation built on earthquake stress transfer. *Journal of Geophysical Research, 110*(B5S16), 1–16.

Wang, H., Wright, T. J., & Biggs, J. (2009). Interseismic slip rate of the northwestern Xianshuihe fault from InSAR data. *Geophysical Research Letters, 36*(3), 1–5.

Wei, M., Sandwell, D., Fialko, Y. (2009). A silent Mw 4.7 slip event of October 2006 on the Superstition Hills fault, southern California. *Journal of Geophysical Research: Solid Earth, 114*(B7)

Wells, D. L., & Coppersmith, K. J. (1994). New empirical relationships among magnitude, rupture length, rupture width, rupture area, and surface displacement. *Bulletin of the Seismological Society of America, 84*(4), 974–1002.

Wen, X. Z. (2000). Character of rupture segmentation of the Xianshuihe- Anninghe- Zemuhe fault zone. *Western Sichuan. Seismology and Geology (in Chinese), 22*(3), 239–249.

Wensnousky, S. G. (1986). Earthquake quaternary faults, and seismic hazard in California. *Journal of Geophysical Research, 91*(B12), 12587–12631.

Wu, P. P., Li, Z., Li, D. H., & Gao, E. G. (2014). Numerical simulation of stress evolution on Xianshuihe Fault based on contact element model. *Progress in Geophysics (in Chinese), 29*(5), 2084–2091.

Xu J. (2013). Tectonic loading and the interacition among the large earthquake on Xianshuihe fault. Institute of Seismic Science, China Earthquake Administration, thesis for master's degree **(in Chinese)**.

Xu, J., Shao, Z. G., Ma, H. S., & Zhang, L. P. (2013). Evolution of Coulomb stress and stress interaction among strong earthquake along the Xianshuihe fault zone. *Chinese J. Geophys. (in Chinese), 56*(4), 1146–1158.

Yi, G. X., Long, F., Wen, X. Z., Liang, M. J., & Wang, S. W. (2015). Seismogenic structure of the M6.3 Kangding earthquake sequence on 22 Nov. 2014, Southwestern China. *Chinese Journal of Geophysics (in Chinese), 58*(4), 1205–1219.

Zhang, X., Tang, H. T., Li, R. S., & Jia, P. (2012). Research on activity features of Xianshuihe fault and its relationship with great earthquakes based upon grey relation degree method. *Journal of seismological research (in Chinese), 35*(4), 500–505.

Zhang, Q. W., Zhang, P. Z., Wang, C., Wang, Y. P., & Ellis, M. A. (2003). Earthquake triggering and delaying caused by fault interaction on Xianshuihe fault belt, southwestern China. *Acta Seismologica Sinica (in Chinese), 25*(2), 143–153.

Zhou, H. L., Allen, C. R., & Kanamori, H. (1983a). Rupture complexity of the 1970 Tonghai and 1973 Luhuo earthquakes, China, from P-Wave inversion, and relationship to surface

faulting. *Bulletin of the Seismological Society of America., 73*(6A), 1585–1597.

Zhou, R. J., He, Y. L., Huang, Z. Z., Li, X. G., & Yang, T. (2001). The slip rate and strong earthquake recurrence interval on the Qianning-Kangding segment of the Xianshuihe fault zone. *Acta Seismologica Sinica (in Chinese), 23*(3), 250–261.

Zhou, H. L., Liu, H. L., & Kanamori, H. (1983b). Source processes of large earthquakes along the Xianshuihe fault in southwestern China. *Bulletin of the Seismological Society of America, 73*(2), 537–551.